Aust. J. Phys., 1987, **40**, 789–800

Models for the Emission Line Spectra of Oxygen-rich Supernova Remnants*

Michael A. Dopita

Mt Stromlo and Siding Spring Observatories, Australian National University, Private Bag, Woden Post Office, A.C.T. 2606, Australia.

Abstract

The mechanism of excitation of the oxygen-rich class of young supernova remnants (SNRs), typified by the fast-moving knots of Cas A, is not currently understood. In this paper we review the available optical data and the current state of attempts at theoretical modelling. A new model is proposed which dramatically improves the fit of the theory with the observations for this class of SNRs. The model is of an X-ray driven R-type ionisation front precursor of a very fast shock. The peculiarities of the thermal balance in oxygen allow an enormous amount of superheating in the gas, which is first exposed to the X-ray ionising field, and the optical emission occurs in this superheated gas. The fit with observation is sufficiently good to give some degree of confidence that the mode of excitation of the plasma has at last been identified, and elemental abundances in four young oxygen-rich SNRs are derived.

1. Introduction

Within the limitations of the assumption of one-dimensional steady flow, it is safe to say that the theoretical modelling of the optical, IR and UV spectra of 'normal' radiative shock waves has reached a level of maturity. Since the pioneering work of Cox (1972), theoretical advances have included the computation of the time dependent ionisation in the post-shock gas (Dopita 1976, 1977; Raymond 1979), the development of self-consistent pre-ionisation models (Shull and McKee 1979), electron–ion relaxation (Ohtani 1980), dust destruction processes (Shull 1978; Draine 1981) and the systematic investigation of the effects of differing heavy element abundances on the output spectra (Dopita *et al.* 1984*a*).

The situation with regard to the young oxygen-rich SNRs is much less satisfactory. It is certain that the composition of the gas approximates to almost pure oxygen, and that this material was expelled by an exploding massive star. It has been assumed that the emission is the result of radiative shocks moving into this material. However, the first realistic models have failed to confirm this assumption (Dopita *et al.* 1984*b*).

In this paper, I review the available observational material on this class of SNRs, and propose new theoretical models. These models are in much better agreement with observations than their predecessors.

* Paper presented at the Joint USSR–Australia Shklovskii Memorial Symposium on Supernova Remnants and Pulsars, held at Pushchino, USSR, 8–11 June 1986.

0004-9506/87/060789$02.00

2. Observational Material

There are now several examples of SNRs, both in our own and external galaxies, in which fast-moving material has been identified at optical wavelengths and which appears to be entirely devoid of either hydrogen or helium. Instead, the optical spectrum is dominated by the forbidden lines of oxygen. In addition, forbidden lines of neon have almost always been identified, and in various other remnants, lines of sulfur, argon and calcium have been identified. The prototype of the class is the SNR Cas A, which was the first to be found (Baade and Minkowski 1954), and has certainly been the most intensively studied. Since then, a further example of this class has been found in the southern skies; G292·0+1·8 (Goss *et al.* 1979; Murdin and Clark 1979). Two further examples have been found in the Large Magellanic Cloud (LMC), N132D (Danziger and Dennefeld 1976*a*, 1976*b*) and 0540−69·3 (Mathewson *et al.* 1980). In addition, one remarkable example is known in the Small Magellanic Cloud (SMC), 1E 102·2−7219 (Dopita *et al.* 1981), and another very bright and dense oxygen-rich SNR has been found in NGC 4449 (Balick and Heckman 1978).

The spectra of these objects strongly support the idea that we are seeing fragments of a massive precursor star which are almost entirely uncontaminated by contact or mixing with the interstellar medium. Thus, an understanding of the physical conditions in these objects would be like a Rosetta Stone in our attempts to investigate the nucleosynthetic end-points of the evolution of massive stars. What has so far been learned about these conditions?

Cas A shows two kinds of filament in the optical, each with strikingly different properties. The so-called ‘quasi-stationary flocculi’ are a set of relatively long-lived slow-moving filaments containing hydrogen, but which appear to be over-abundant in nitrogen (Peimbert and van den Bergh 1971; Chevalier and Kirshner 1978). They appear to be shock-excited remnants of a pre-supernova shell. The similarity of composition with the nebula NGC 6888 around a Wolf–Rayet N star has been remarked upon by Parker (1978), suggesting that we are seeing contamination by CN processed material. The system has a radius of 120 arcsec, or 1·6 pc at a distance of 2·8 kpc (van den Bergh 1971; Sakhibov 1980), and appears to be expanding at about 300 $\mathrm{km\,s^{-1}}$ (van den Bergh and Kamper 1985).

The fast-moving knots (FMK) appear to form a system with a velocity of expansion of up to 8500 $\mathrm{km\,s^{-1}}$. They are composed entirely of heavy elements, although the elemental composition appears to change markedly from one filament to the next (Peimbert and van den Bergh 1971; Kirshner and Chevalier 1977; Chevalier and Kirshner 1978, 1979) which suggests that the ejected material has not been well mixed. The proper motions can be used to fix the time of explosion to AD 1658 (van den Bergh and Kamper 1983). However, the individual knots appear to be very ephemeral objects, showing velocity shears of up to about 2000 $\mathrm{km\,s^{-1}}$, and e-folding lifetimes of only about 25 years (Kamper and van den Bergh 1976).

The evolutionary state of the oxygen-rich SNR is one in which the ejecta are not fully thermalised. This is clearly shown by observations of the X-ray structure (Fabian *et al.* 1980). The Einstein Observatory HRI image has two shell-like structures which can be interpreted as the outer blast wave and the inner reverse shock. These have radii of about 140 and 100 arcsec respectively (1·9 and 1·3 pc respectively). Comparison of the ratio of radii with models (Gull 1973) suggests that the ratio of swept-up mass to ejected mass is about unity in this remnant.

It is generally believed that the FMK are excited into emission when they pass through the reverse shock and start to be decelerated from their initial ballistic expansion, although the mode of excitation remains unclear; this will be discussed in the following section. Clumps of matter may be produced either by the action of a Rayleigh–Taylor instability in the deceleration region, or by instability in the early post-supernova phase. Mechanisms which have been proposed include Rayleigh–Taylor instabilities (Chevalier 1975), a thermal instability following the time at which the ejecta become optically thin (Dopita *et al.* 1984*b*) or convective instabilities (Bandiera 1984). The picture in which the knots are formed at an early stage seems to be supported by what we know about the dynamics of the oxygen-rich SNRs. In no case yet studied is the velocity field consistent with an expanding shell of matter. In the case of Cas A (Winkler *et al.* 1982), G 292·0−1·8 (Tuohy *et al.* 1982), N132D (Lasker 1980) and 1E0102·2−7219 (Tuohy and Dopita 1983), the data suggest that the oxygen-rich material is found in a ring shaped structure. This could be explained by a global instability in the supernova event, but not otherwise.

The oxygen-rich SNRs are an exceedingly luminous class of objects at X-ray wavelengths. For example, N132D has a luminosity of $8\cdot3\times10^{37}$ erg s^{-1} in the 0·15–4·5 keV range, and 1E 102·2−7219 has a luminosity of $2\cdot1\times10^{37}$ erg s^{-1} in the same range (Long *et al.* 1981; Seward and Mitchell 1981). The latter object is surrounded by a low-velocity, high excitation halo, which is conceivably photoionised by this X-ray emission (Tuohy and Dopita 1983). These very high luminosities are doubtless the result of both non-equilibrium ionisation conditions, which enhance the X-ray emissivity by an order of magnitude (Hamilton *et al.* 1983) and also because of the enhanced heavy element abundances (Long *et al.* 1982).

The SNR 0540−69·3 has recently been found to be associated with a 50 ms X-ray and optical pulsar (Seward *et al.* 1984; Middleditch and Pennypacker 1985). This must be exceedingly luminous, considering the object is located in the LMC, and is the first direct evidence that a massive star can create a neutron star. It appears to have been born with an unusually low frequency, making it in some respects like the Crab. In addition to the 8 arcsec (2·1 pc) diameter [O III] shell (Mathewson *et al.* 1980), the pulsar excites a synchrotron nebula some 4 arcsec across (Chanan *et al.* 1984).

3. Models for Oxygen-rich SNRs

(a) Radiative Shock-wave Models

The definition of physical conditions in the optically emitting plasmas of the class of oxygen-rich SNRs has been severely hampered by the lack of emission line ratios that can be used for diagnostic purposes (Dopita and Tuohy 1984). The derivation of more reliable limits on the physical conditions and the chemical abundances ought to be possible from a model of the emitting zone. It has generally been assumed, explicity or tacitly, that the optical emission in the oxygen-rich filaments is the result of slow, fully radiative shocks propagating into dense knots of material as they enter the high-pressure regime behind the reverse shock (Peimbert and van den Bergh 1971; Lasker 1978; Chevalier and Kirshner 1978, 1979; Goss *et al.* 1979; Murdin and Clark 1979; Kirshner and Blair 1980).

The first attempt to model this type of system was by Itoh (1981), who showed the very curious structure of shock waves in pure oxygen gas, and who also demonstrated the importance of pre-ionisation. Models with a reasonable mix of elements were constructed by Dopita *et al.* (1984*b*). Although these share many of the properties of the pure oxygen models they differ in several important respects.

Because oxygen is such an efficient coolant, these models show several pathological features. Firstly, the ion and electron temperatures are rarely similar. In the early part of the post-shock flow, the electron temperature T_e is much lower than the ion temperature T_i. As superelastic collisions transfer energy to the electron gas, T_e rapidly rises. However, when the temperature reaches $(1–2)\times 10^5$ K, the inelastic collisions lose as much energy as is gained from superelastic collisions, and T_e changes rather slowly throughout the bulk of the cooling zone. As T_e and T_i draw together, the approximately isobaric compression causes a rapid increase in the volume emissivity of the plasma and consequent rapid decrease in the temperature. In a pure oxygen plasma, the instantaneous cooling time-scale remains shorter than the recombination time-scale until temperatures of order 100 K are reached, and the fine structure cooling in IR lines is finally quenched. Thus, the temperature suffers a catastrophic collapse with 'frozen-in' ionisation state.

The high emissivity of the hot zone has another consequence. A very large number of ionising photons are emitted, which leak out of the leading and trailing edges of the shock front to pre-ionise the gas, mainly to O II, and to heat the recombination zone to over 1000 K. In pure oxygen gas, these photoionised zones contribute appreciably to the total emission. However, if other elements are included, the increased IR cooling ensures an equilibrium temperature which cannot exceed about 100 K.

With the structure described above, radiative shock-wave models can never adequately describe the observed spectra. Because of the initial ionisation, no model produces appreciable [O I]. Since the electron temperature rapidly rises to about 10^5 K, the [O III] ratio 4363 Å/5007 Å is about twice as high in the models as is observed. Furthermore, the output spectrum is a sensitive function of the shock velocity. In order to produce the correct [O III]/[O II] line ratios, and also the correct [Ne V]/[Ne III] ratios, the shock velocity would have to be between 100 and 130 km s^{-1} in *all* remnants. This seems most unphysical, given the variation in other properties between the remnants.

(b) Photoionisation Precursor Model

Dopita *et al.* (1984*b*) considered that the relatively small variations in levels of excitation within and between remnants implied a common excitation source. Furthermore, the presence of [O I] implies a local source of heating, since without it, the temperature would be around 100 K and the forbidden line quenched. Three possibilities were briefly considered, electron conduction, heating by suprathermal particles and photoionisation by X rays. Here we develop the last idea.

As described above, a shock front in oxygen-rich gas is a copious source of pre-ionising photons. At shock velocities of about 120 km s^{-1}, these are not very hard, and the preionisation only goes as far as O III. However, clumps of oxygen-rich matter pass through the reverse shock at velocities of between 2000 and 4000 km s^{-1}, and the pressure at the stagnation point may be as high as three times the ram pressure of the surrounding intercloud medium, so that a shock is driven into the cloud at a velocity of approximately $5000(n_i/n_c)^{1/2}$ km s^{-1}, where n_i is the density of the intercloud medium and n_c is the density of the cloud. Assuming a generous density contrast of order 1 : 100, we would get shock velocities of order 500 km s^{-1}, or post-shock temperatures of order 10^8 K. Such high shock velocities would effectively ensure that the shock would not become fully radiative, but that instead, the cloudlet would be ablated from the outside. Furthermore, at such high temperatures, ionisation is very rapid until the hydrogen and helium-like ions are the dominant ions. The X-ray emissivity would in consequence be very strongly enhanced for these species (see e.g. Hamilton and Sarazin 1984). Thus a cloudlet entering the reverse shock will develop an X-ray emitting halo which will bathe the unshocked part in a 'hard' (200–2000 eV) photon field of rapidly increasing intensity.

The consequences of such a photon field will be to cause the development of an ionisation front ahead of the shock. As the supply of photons increases, the front will accelerate. Could such an R-type ionisation front emit a significant amount of optical radiation? To test this possibility, I have constructed models of such an ionisation front, using the same generalised modelling code MAPPINGS as in our earlier work (e.g. Dopita *et al.* 1984*a*, 1984*b*).

The dominant emission lines in the post-shock gas will be Ne X; 1305, 1285, 1210, 1010 eV; Ne IX; 1192, 1126, 1072, 922, 914, 904 eV; Ne VIII; 1072 eV; Ne VI; 880 eV; O VIII; 835, 822, 774, 646 eV; O VII; 714, 698, 666, 574, 561 eV and O VI; 562, 463, 436 eV. In addition, the plasma will emit an underlying bound–free and free–free continuum. Non-equilibrium spectra have been calculated by Hamilton *et al.* (1983). In order to give a simple parametric fit to these very complex X-ray spectra, these have been approximated by power laws with a spectral index α between -1 and -4, with or without a high frequency cut at 100 Ryd (1 Ryd $\equiv 3\cdot29\times10^{15}$ Hz).

The models are then defined by the specific intensity of the radiation field or, equivalently, the velocity of the ionisation front. For all reasonable ionisation front velocities (100–5000 km s^{-1}), the equilibrium temperature is very low (100–300 K). However in an ionisation front, the un-ionised plasma is suddenly immersed in a strong radiation field. Each photoionisation on average deposits of order 200–500 eV in the plasma, and initially the cooling rate by inelastic collisions of electrons is very low. Thus, the electron temperature rises very rapidly. A maximum temperature is reached when the photoionisation heating rate matches the radiative losses in the plasma, after which the temperature falls back towards its equilibrium value.

The maximum superheating achieved is a sensitive function of the ionisation front velocity, and is somewhat less dependent on the shape of the ionising spectrum and the composition of the gas. Fig. 1 shows the dependence of the maximum temperature T_{max}, and the time taken to reach this temperature t_{max}, as a function of ionisation front velocity v_I. This has been computed for an ionising spectrum of index -2 between 1 and 100 Ryd, moving into a plasma with a composition O : Ne $= 1\cdot0:0\cdot39$ by number and with an oxygen atom density of $n(\mathrm{O}) = 100$ cm^{-3}. For velocities in excess of 1000 km s^{-1}, the peak temperature exceeds 20 000 K, a temperature that is required if the observed emission line ratios are to be explained (Dopita and Tuohy 1984). In fact, maximum electron temperatures may be in excess of what we have calculated because our models assume ion–electron equipartition, and in such a situation of rapid heating of the electron gas, the ion temperature can be expected to lag behind.

Two compositions of the plasma have been assumed. In model R1 the element mixture (abundance set M) given by Dopita *et al.* (1984*b*) has been used, while model R2 uses the ratio O : Ne = 1·0 : 0·39 and zero abundance of other elements. Because of lower electron densities and fewer channels for cooling, the maximum temperatures reached for the 'pure' O–Ne mixtures are higher than for mixture M with the same ionisation front velocity. For model R1 an untruncated ionisation spectrum of index −2·0 is assumed, with an ionisation front velocity of 2900 km s^{-1}. Model R2 takes a power law spectrum of index −2·0 and truncates at 100 Ryd, and has an ionisation front velocity of 2000 km s^{-1}. The results for these models are compared with the shock-wave models and the observations on Magellanic Cloud oxygen-rich SNRs in Table 1.

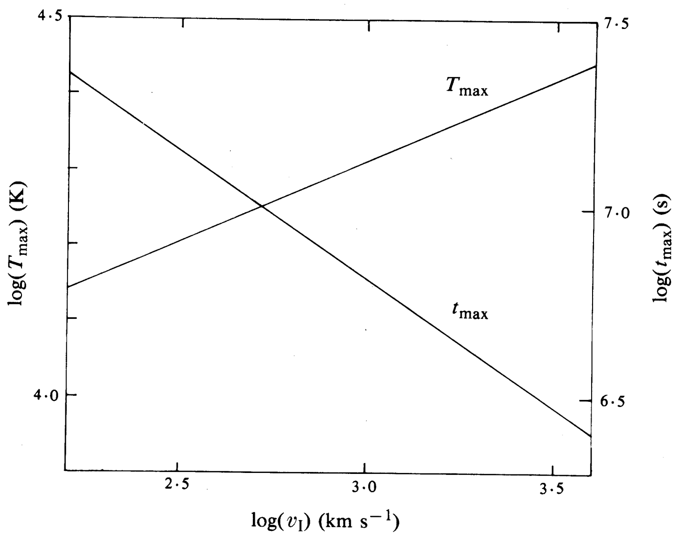

Fig. 1. Maximum temperature and the time taken to reach this temperature as a function of the R-type ionisation front velocity. The oxygen atom density is n(O) = 100 cm^{-3}, the elemental composition is O : Ne = 1·0 : 0·39 and the power law index of the ionising spectrum is −2·0 (1–100 Ryd).

The very sharp increase in the electron temperature, and its slower decline towards the equilibrium value as the ionisation state gets closer to its equilibrium value, is graphically shown in Fig. 2 for model R1. The volume emissivities of five important oxygen lines are shown in Fig. 3. Since, at a given ionisation parameter (the number of ionising photons per atom), the cooling time-scale scales as the density, changes in the physical conditions should scale as the product of real time and oxygen density over a fairly wide range of densities.

The surface luminosities achieved in these models are considerable. For both R1 and R2 the luminosity in the [O III] λ5007 Å line is close to 10^{-2} erg cm^{-2} s^{-1} sr^{-1}. On the other hand, because the temperatures are nowhere near as high as those reached in the shock models, the UV lines are predicted to be comparatively weak. For model

R2, the intensities of the UV oxygen lines on the scale [O III] λ5007 Å = 100·0 are as follows:

$$[\mathrm{O\,I}]\ \lambda 1357\ \text{Å} = 11{\cdot}24; \qquad [\mathrm{O\,II}]\ \lambda 2470\ \text{Å} = 7{\cdot}6;$$

$$[\mathrm{O\,III}]\ \lambda 1664\ \text{Å} = 2{\cdot}31; \qquad [\mathrm{O\,IV}]\ \lambda 1403\ \text{Å} = 0{\cdot}15.$$

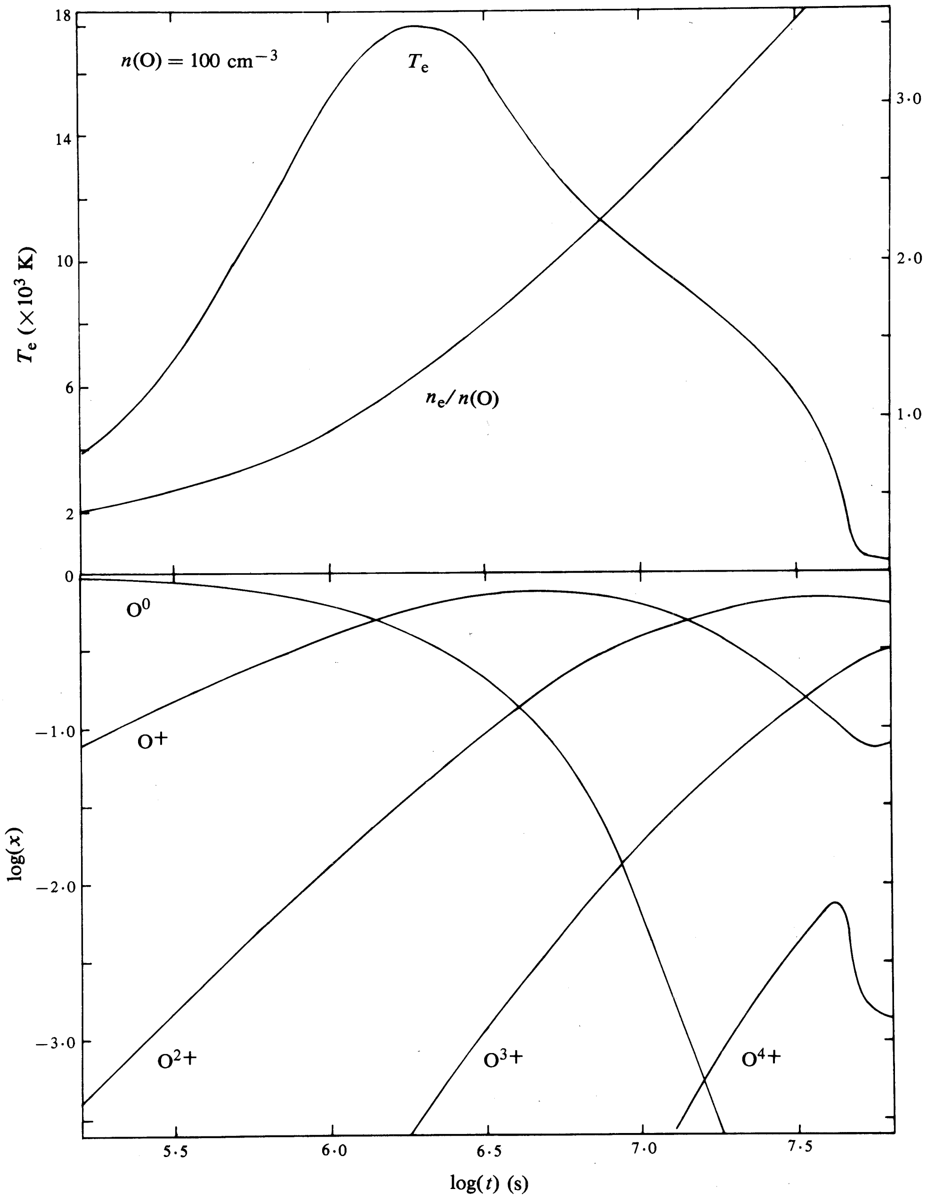

Fig. 2. Temperature and ionisation structure of the R-type ionisation front R1, as described in Section 3*b*.

Table 1. **Comparison of radiative shock models (Dopita *et al.* 1984*b*), shock-driven R-type ionisation front models, and the observed spectra of Magellanic Cloud oxygen-rich SNRs**

Logarithmic line ratio	Shock models S3A	Shock models S2C	I-front models R1	I-front models R2	Observed Mag. Cloud SNRs 0540	Observed Mag. Cloud SNRs N132D	Observed Mag. Cloud SNRs 1E 0102·2
[O III] λ4363/[O III] λ5007	−0·93	−1·22	−2·16	−1·93	−1·5	−1·4	−1·4
[O II] λ7325/[O II] λ3727, 9	−1·03	−1·19	−1·42	−1·41	< −1·4	−1·3	< −1·4
[Ne III] λ3868/[O III] λ5007	−0·96	−0·82	−1·14	−1·14	—	−1·0	−0·9
[O II] λ3727, 9/[O I] λ6300	+2·81	+2·19	+1·50	+1·47	+1·3	+1·3	+1·7
[O III] λ5007/[O II] λ3726, 9	−0·36	+0·03	−0·12	−0·42	+0·3	−0·3	−0·1
[Ne V] λ3426/[Ne III] λ3868	< −3·0	−2·88	−3·05	−3·49	—	< −0·5	−0·6

Table 2. **Inferred chemical composition of young SNRs measured by Dopita and Tuohy (1984)**

Object name	O	Ne	Mg	S	Ar
G 292·0+1·8	10 000	3700	—	<30	—
0540−69·3	10 000	<800	<500	620	65:
N132D	10 000	4890	<220	<30	—
1E 0101·2−7219	10 000	9240	<220	<4	<5

The UV data from space observatories such as HST should provide a stringent test of the theory. These data would be useful in another regard. If the elements C, Si and Mg are present at an appreciable abundance with respect to O, then they would be detectable only in the 1300–3000 Å portion of the spectrum, and would provide a great deal of new information on the nucleosynthetic processes of massive stars.

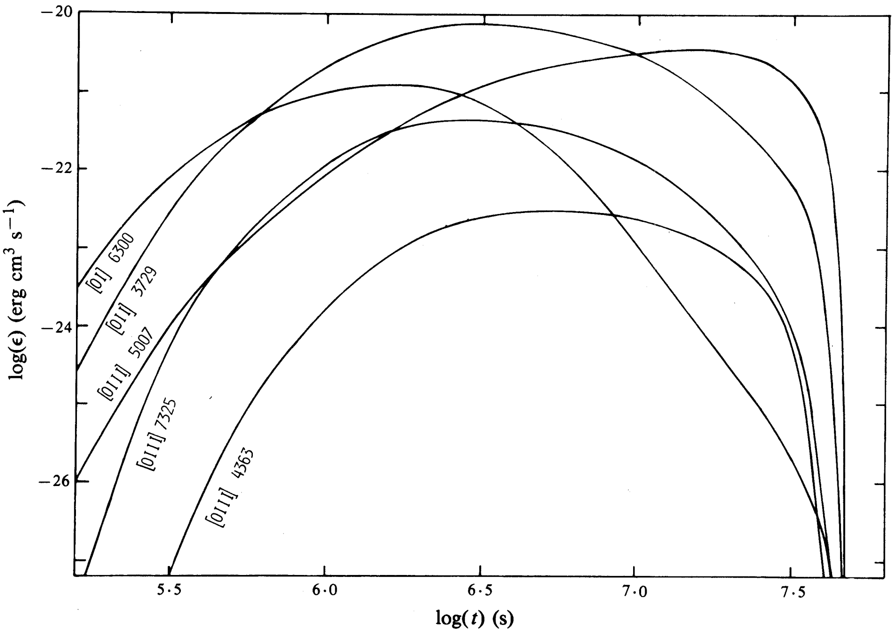

Fig. 3. Evolution of emissivity ε of five important oxygen lines in model R1.

These ionisation front models represent a notable improvement in the fitting of the observed spectra. Not only are the [O I] : [O II] : [O III] ratios close to those observed, but the computed temperatures of the [O II] and [O III] zones, as given by the first two ratios of Table 1, are close to those which are observed. The fact that the λ4363 Å value (first row in Table 1) is somewhat underestimated probably reflects the fact that, in the real world, the electron gas is somewhat hotter than the ions. The extent of the accord between the observed and computed ionisation and temperature structures is encouraging, and suggests that the correct mode of excitation has been identified. By way of further support for the model, we recall that in Cas A the individual knots or knot complexes are 2–10 arcsec across (0·03–0·15 pc). Assuming an ionisation front velocity of 2000 km s^{-1}, the front would pass entirely through the knots in 15–75 years. This is consistent with the observed lifetimes of about 25 years (Kamper and van den Bergh 1976), and is a further indication that the proposed mechanism may indeed be correct. The Ne IV and Ne V line strengths may also be accounted for with a sufficiently high shock velocity (see Section 4).

(c) Estimation of the Elemental Composition of Observed SNRs

If we accept the proposed mechanism as the method of excitation of the plasma, then the relative abundances of the elements can be estimated on the basis that the intensity with respect to any oxygen ion scales as the relative abundance of the element with respect to oxygen. From Table 1, it is evident that this is indeed the case, at least as far as the ratio [Ne III]/[O III] is concerned. In Table 2, the abundances have been derived on the assumption that the intensities of dominant emission lines such as [S II] λ6717, 31 Å, [Ar III] λ7135 Å, [Ar IV] λ4711 Å and [Mg I] λ4568 Å scale from model R1 as the abundance.

It is clear that there exist considerable variations in chemical composition from one remnant to another. This suggests that the ejecta are not well mixed. This viewpoint finds support when the abundances of Table 2 are compared with the theoretical computations for the end-point of the evolution of massive stars by Woosley and Weaver (1981). The neon-to-oxygen ratios of G 292·0+1·8 and N132D are consistent with the hypothesis that we are seeing the helium-burnt layers of a star of initial mass of order 25 solar masses. The high neon abundance in 1E 0101·2−7219 suggests a rather less massive precursor. In each of these three cases, the limits on Mg, S and Ar prove that the layers close to the neutronised core are not mixed in, and the complete absence of H or He proves that there has been no contamination by the outer layers, or by the interstellar medium. The case of 0540−69·3 is very interesting. The absence of Ne means that the material must have originated in the inner part of the star where oxygen burning had started. This is also suggested by the high S abundance, and the suggestion that Ar may be present. A mixture similar to this object was obtained in the theoretical model of Woosley and Weaver (1981), provided only the zone 1·7–2·0 solar masses of a 25 solar mass precursor is involved. The inner part of such a zone is also rich in Ca, and this is consistent with the identification of [Ca I] λ6573 Å emission. However, it is unclear why only the singly ionised species is identified. This line may not, however, be excited in the same way as the others. The diameter of the Ca line emitting shell is smaller than the O-emitting region (Mathewson *et al.* 1980), and is similar in size to the synchrotron nebula (Chanan *et al.* 1984). It is therefore probable that it is excited by the synchrotron emission associated with the optical pulsar, rather than by an ionising precursor.

4. Conclusions

This study has established that the mechanism of excitation of the fast-moving optically emitting material in young oxygen-rich SNRs is probably superheating in an R-type ionisation front precursor of a fast X-ray emitting shock. The mechanism can reproduce the excitation and temperature of the observed plasma, and these results can be used to estimate, for the first time, relatively reliable chemical abundances.

These models are capable of considerable further refinement. The true X-ray spectrum, and its development with time as the fast shock propagates into the oxygen-rich clump, should be calculated. This would permit a more accurate solution of the time dependent ionisation problem, and also allow us to study the details of the acceleration of the ionisation front into the dense clouds. Finally, the assumption of ion–electron equipartition should be abandoned. The heating of the electron gas would then be more rapid than the ionic heating, and the peak temperatures reached may be considerably higher for a given ionisation front velocity. This is likely to explain the difference in the [O III] temperature between the models presented here and the observations. With a sufficiently high ionisation front velocity, the collisional ionisation rate might become comparable with the photoionisation rate, so that the presence of appreciable [Ne IV] and [Ne V] emission in 1E 0102·2−7219 might be correctly accounted for.

References

Baade, W., and Minkowski, R. (1954). *Astrophys. J.* **119**, 206.
Balick, B., and Heckman, T. (1978). *Astrophys. J. Lett.* **226**, L7.
Bandiera, R. (1984). *Astron. Astrophys.* **139**, 368.
Chanan, G. A., Helfand, D. J., and Reynolds, S. P. (1984). *Astrophys. J. Lett.* **287**, L23.
Chevalier, R. A. (1975). *Astrophys. J.* **200**, 698.
Chevalier, R. A., and Kirshner, R. P. (1978). *Astrophys. J.* **219**, 931.
Chevalier, R. A., and Kirshner, R. P. (1979). *Astrophys. J.* **233**, 154.
Cox, D. P. (1972). *Astrophys. J.* **178**, 143.
Danziger, I. J., and Dennefeld, M. (1976*a*). *Publn Astron. Soc. Pacific* **88**, 44.
Danziger, I. J., and Dennefeld, M. (1976*b*). *Astrophys. J.* **207**, 394.
Dopita, M. A. (1976). *Astrophys. J.* **209**, 395.
Dopita, M. A. (1977). *Astrophys. J. Suppl. Ser.* **37**, 117.
Dopita, M. A., Binette, L., D'Odorico, S., and Benvenuti, P. (1984*a*). *Astrophys. J.* **276**, 653.
Dopita, M. A., Binette, L., and Tuohy, I. R. (1984*b*). *Astrophys. J.* **282**, 142.
Dopita, M. A., and Tuohy, I. R. (1984). *Astrophys. J.* **282**, 135.
Dopita, M. A., Tuohy, I. R., and Mathewson, D. S. (1981). *Astrophys. J. Lett.* **248**, L105.
Draine, B. T. (1981). *Astrophys. J.* **245**, 880.
Fabian, A. C., Willingale, R., Pye, J. P., Murray, S. S., and Fabbiano, G. (1980). *Mon. Not. R. Astron. Soc.* **193**, 175.
Goss, W. M., Shaver, P. A., Zealey, W. J., Murdin, P., and Clark, D. H. (1979). *Mon. Not. R. Astron. Soc.* **188**, 357.
Gull, S. F. (1973). *Mon. Not. R. Astron. Soc.* **161**, 47; **162**, 135.
Hamilton, A. J. S., and Sarazin, C. L. S. (1984). *Astrophys. J.* **284**, 601.
Hamilton, A. J. S., Sarazin, C. L. S., and Chevalier, R. A. (1983). *Astrophys. J. Suppl. Ser.* **51**, 115.
Itoh, H. (1981). *Publn. Astron. Soc. Jpn* **33**, 121; 521.
Kamper, K. W., and van den Bergh, S. (1976). *Astrophys. J. Suppl. Ser.* **32**, 351.
Kirshner, R. P., and Blair, W. P. (1980). *Astrophys. J.* **236**, 135.
Kirshner, R. P., and Chevalier, R. A. (1977). *Astrophys. J.* **218**, 142.
Lasker, B. M. (1978). *Astrophys. J.* **223**, 109.
Lasker, B. M. (1980). *Astrophys. J.* **237**, 765.
Long, K. S., Dopita, M. A., and Tuohy, I. R. (1982). *Astrophys. J.* **262**, 202.
Long, K. S., Helfand, D. J., and Grabelsky, D. A. (1981). *Astrophys. J.* **248**, 925.
Mathewson, D. S., Dopita, M. A., Tuohy, I. R., and Ford, V. L. (1980). *Astrophys. J. Lett.* **242**, L73.
Middleditch, J., and Pennypacker, C. (1985). *Nature* **313**, 959.
Murdin, P., and Clark, D. H. (1979). *Mon. Not. R. Astron. Soc.* **189**, 501.
Ohtani, H. (1980). *Publn Astron. Soc. Jpn* **32**, 11.
Parker, R. A. R. (1978). *Astrophys. J.* **224**, 873.
Peimbert, M., and van den Bergh, S. (1971). *Astrophys. J.* **167**, 223.
Raymond, J. C. (1979). *Astrophys. J. Suppl. Ser.* **39**, 1.
Sakhibov, F. K. (1980). *Sov. Astron. Lett.* **6**, 56.
Seward, F. D., Harnden, F. R., and Helfand, D. J. (1984). *Astrophys. J. Lett.* **287**, L19.
Seward, F. D., and Mitchell, M. (1981). *Astrophys. J.* **243**, 736.
Shull, J. M. (1978). *Astrophys. J.* **226**, 858.
Shull, J. M., and McKee, C. F. (1979). *Astrophys. J.* **227**, 131.
Tuohy, I. R., Clark, D. H., and Burton, W. M. (1982). *Astrophys. J. Lett.* **268**, L65.
Tuohy, I. R., and Dopita, M. A. (1983). *Astrophys. J. Lett.* **268**, L11.
van den Bergh, S. (1971). *Astrophys. J.* **165**, 457.
van den Bergh, S., and Kamper, K. W. (1983). *Astrophys. J.* **268**, 129.
van den Bergh, S., and Kamper, K. W. (1985). *Astrophys. J.* **293**, 537.

Winkler, P. F., Canizares, C. R., Markert, T. H., and Szymkowiak, A. E. (1982). *In* 'Supernovae: A Survey of Current Research' (Eds M. J. Rees and R. J. Stoneham), p. 501 (Cambridge Univ. Press).

Woosley, S. E., and Weaver, T. A. (1981). *In* 'Essays in Nuclear Astrophysics' (Eds C. A. Barnes *et al.*), p. 377 (Cambridge Univ. Press).

Manuscript received 16 April, accepted 24 June 1987